

# Silane Activation by $\text{Ti}(\text{NMe}_2)_4$ and $\text{NH}_3$ during Chemical Vapor Deposition of Ti–Si–N Films

Carmela C. Amato-Wierda,\* Edward T. Norton, Jr., and Derk A. Wierda†

Materials Science Program, Parsons Hall, University of New Hampshire,  
Durham, New Hampshire 03824

Received March 24, 1999. Revised Manuscript Received June 30, 1999

Molecular beam mass spectrometry has been used to observe the activation of silane, predominantly in the gas phase, during the chemical vapor deposition of Ti–Si–N thin films using  $\text{Ti}(\text{NMe}_2)_4$ , tetrakis(dimethylamido)titanium, silane, and ammonia at 450 °C. The extent of silane reactivity was dependent upon the relative amounts of  $\text{Ti}(\text{NMe}_2)_4$  and  $\text{NH}_3$ . Ti–Si–N thin films were deposited using similar process conditions as the molecular beam experiments. RBS and XPS were used to determine the atomic composition of these films. The variations of the Ti:Si ratio as a function of  $\text{Ti}(\text{NMe}_2)_4$  and  $\text{NH}_3$  flows were consistent with the changes in silane reactivity under similar conditions.

## Introduction

Ti–Si–N is a refractory amorphous ternary nitride which is a promising candidate for diffusion barrier applications in future metallization schemes of integrated circuits.<sup>1–4</sup> These films also show potential as nanophase materials with improved mechanical properties.<sup>5–7</sup>

Two chemical vapor deposition (CVD) processes have been used to make Ti–Si–N films. One process reacts  $\text{TiCl}_4$  along with  $\text{SiCl}_4$  or  $\text{SiH}_2\text{Cl}_2$ ,  $\text{NH}_3$ , and  $\text{H}_2$  above 1000 °C.<sup>6,7</sup> This method is most appropriate for refractory coatings, such as hard coatings on cutting tools, where high temperatures are not deleterious to the substrate. Plasma-enhanced CVD with these precursors lowers the deposition temperature to 560 °C.<sup>5</sup> Alternatively, the  $\text{Ti}(\text{NR}_2)_4$  (R = Me or Et),  $\text{NH}_3$ , and  $\text{SiH}_4$  precursor system enables deposition of Ti–Si–N films at temperatures below 450 °C, which is low enough for

microelectronics applications.<sup>1,4</sup> The  $\text{Ti}(\text{NR}_2)_4$  (R = Me or Et) +  $\text{NH}_3$  process (without the silane) has been extensively studied because it is used to deposit TiN in the semiconductor industry.<sup>8–15</sup>

In the case of the  $\text{Ti}(\text{NR}_2)_4$  system, it is interesting that silane reacts at these low temperatures given that silane and ammonia typically require temperatures between 600 and 700 °C to form  $\text{Si}_3\text{N}_4$ .<sup>16</sup> This suggests that silane reactivity, and therefore silicon incorporation into the films, is facilitated by the presence of  $\text{Ti}(\text{NR}_2)_4$ . Both the electrical and mechanical properties of Ti–Si–N films depend strongly on their silicon content. Therefore, it is important to determine if gas-phase chemistry controls silicon incorporation into these films.

Using molecular beam mass spectrometry, we have demonstrated that silane is activated, predominantly in the gas phase, by  $\text{Ti}(\text{NMe}_2)_4$ , tetrakis(dimethylamido)titanium (TDMAT) and ammonia at 450 °C during the CVD of Ti–Si–N films. More importantly, we have correlated the extent of this silane reaction under several conditions to variations in atomic composition in Ti–Si–N deposited by thermal CVD.

## Experimental Section

The experimental apparatus, shown schematically in Figure 1, is a high-temperature flow reactor coupled to a four-stage

\* To whom correspondence should be addressed.

† Present address: Chemistry Department, Saint Anselm College, Manchester, NH 03102.

(1) Smith, P. M.; Custer, J. S. *Appl. Phys. Lett.* **1997**, *70*, 3116–3118.

(2) Reid, J. S. Amorphous ternary diffusion barriers for silicon metallizations. Ph.D. Thesis, California Institute of Technology, May, 1995.

(3) (a) Sun, X.; Reid, J. S.; Kolawa, E.; Nicolet, M. A. *J. Appl. Phys.* **1997**, *81*, 656–663. (b) Sun, X.; Reid, J. S.; Kolawa, E.; Nicolet, M. A. *J. Appl. Phys.* **1997**, *81*, 664–671.

(4) Raaijmakers, I. J. *Thin Solid Films* **1994**, *247*, 85–93.

(5) Shizhi, L.; Yulong, S.; Hongrui, P. *Plasma Chem. Plasma Process.* **1992**, *12*, 287–297.

(6) (a) Toshio, H.; Shinsuke, H. *J. Mater. Sci.* **1982**, *17*, 1320–28. (b) Shinsuke H.; Toshio H.; Kenji H.; Makoto H. *J. Mater. Sci.* **1982**, *17*, 3336–3340. (c) Toshio, H.; Shinsuke, H. *J. Mater. Sci.* **1983**, *18*, 2401–2406.

(7) Llauro, G.; Hillel, R.; Sibieude, F. *Chem. Vap. Deposition* **1998**, *4*, 247–252.

(8) Sugiyama, K.; Pac, Sangryul, P.; Takahashi, Y.; Motojima, S. *J. Electrochem. Soc.* **1975**, *122*, 1545–1549.

(9) (a) Fix, R. M.; Gordon, R. G.; Hoffman, D. M. *Chem. Mater.* **1990**, *2*, 235–241. (b) Fix, R. M.; Gordon, R. G.; Hoffman, D. M. *Chem. Mater.* **1991**, *3*, 1138–1148. (c) Musher, J. M.; Gordon, R. G. *J. Mater. Res.* **1996**, *11*, 989–1001. (d) Musher, J. M.; Gordon, R. G. *J. Electrochem. Soc.* **1996**, *143*, 736–744. (e) Hoffman, D. M. *Polyhedron* **1994**, *13*, 1169–1179.

(10) (a) Katz, A.; Feingold, A.; Pearton, S. J.; Nakahara, S.; Ellington, M.; Chakrabarti, U. K.; Geva, M.; Lane, E. *J. Appl. Phys.* **1991**, *70*, 3666–3677. (b) Katz, A.; Feingold, A.; Nakahara, S.; Pearton, S. J.; Lane, E.; Geva, M.; Stevie, F. A.; Jones, K. *J. Appl. Phys.* **1992**, *15*, 993–1000.

(11) Sun, S. C.; Tsai, M. H. *Thin Solid Films* **1994**, *253*, 440–444. (12) Paranjpe, A.; IslamRaja, M. *J. Vac. Sci. Technol. B* **1995**, *13*, 2105–2114.

(13) Truong, C. M.; Chen, P. J.; Corneille, J. S.; Oh, W. S.; Goodman, D. W. *J. Phys. Chem.* **1995**, *99*, 8831–8842.

(14) (a) Dubois, L. H.; Zegarski, B. R.; Girolami, G. S. *J. Electrochem. Soc.* **1992**, *139*, 3603–3609. (b) Prybyla, J. A.; Chiang, C.-M.; Dubois, L. H. *J. Electrochem. Soc.* **1993**, *140*, 2695–2702. (c) Dubois, L. H. *Polyhedron*, **1994**, *13*, 1329–1336.

(15) (a) Weiler, B. H.; *Chem. Mater.* **1995**, *7*, 1609–1611. (b) Weiler, Bruce H. *J. Am. Chem. Soc.* **1996**, *118*, 4975–4983.

(16) Pierson, Hugh O. *Handbook of Chemical Vapor Deposition: Principles, Technology and Applications*; Noyes Publications: Park Ridge, New Jersey, 1992.

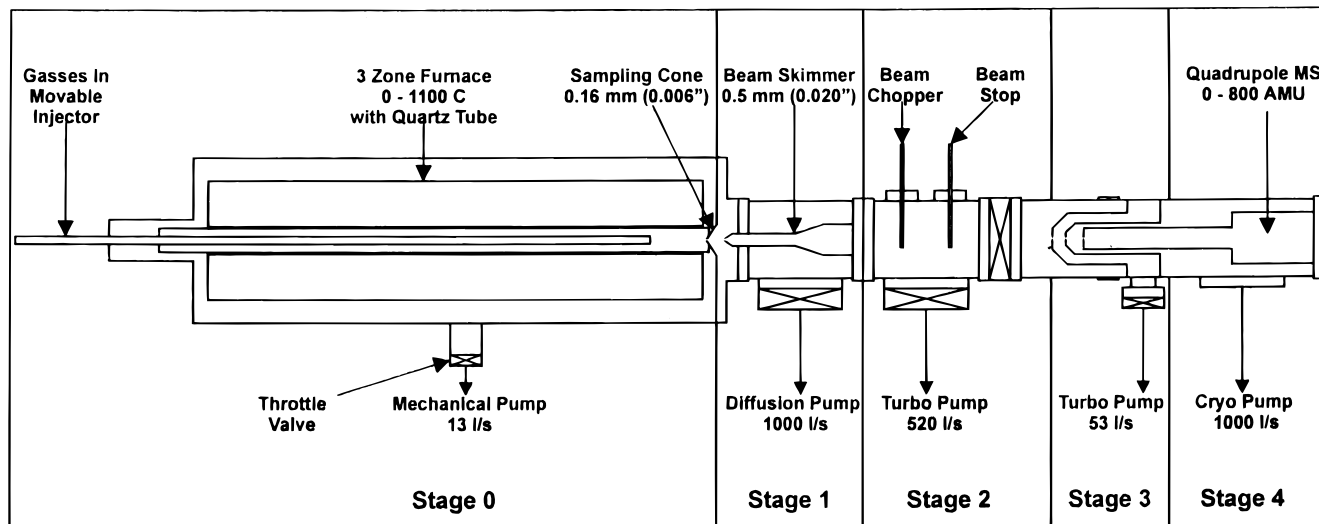


**Figure 1.** Schematic of molecular beam mass spectrometer coupled to the high-temperature flow/CVD reactor.

differentially pumped molecular beam mass spectrometer. The flow reactor is a water-cooled stainless steel vacuum chamber that contains a quartz tube inside a three-zone, resistively heated furnace. The quartz tube has an inside diameter of 3.8 cm and a length of 61 cm. The temperature of each zone is independently controlled by a feedback loop using type-K thermocouples. A moveable injector with translation along the axis of the quartz tube is used to generate kinetic data.

A conical aperture at the end of the reactor samples the gas flow during CVD and forms it into a molecular beam. The beam is skimmed and collimated before entering the ion source of a quadrupole mass spectrometer. The mass spectrometer signals are collected at various  $m/e$  values by a multichannel scaler data acquisition card synchronized to the frequency of a mechanical chopper in the beam path. In the experiments below, the silane (mass = 32) is monitored at  $m/e = 30$  (parent ion minus two hydrogen atoms) because this is the most intense peak in the silane mass spectrum. The silane signals are normalized to argon as an internal standard to account for drifting instrument sensitivity. This normalized silane signal is proportional to the concentration of silane in the gas phase. The instrument's detection limit for silane is 200 ppm.

A gas inlet system meters gas flows to the reactor and consists of mass flow controllers, a TDMAT bubbler, pressure control valves, and capacitance manometers. Gases include TDMAT, argon carrier and diluent gas, ammonia, and silane (1.5% in Ar). The reactor pressure is regulated by a feedback-controlled throttle valve on the exhaust port. For all experiments, the reactor temperature is 450 °C, reactor pressure is 6.5 Torr, and the total gas flow rate is 785 sccm, which corresponds to a residence time of 35 ms under the laminar flow conditions used in this work.

## Results

Figure 2 shows the percent silane reacted as a function of varying  $\text{Ti}(\text{NMe}_2)_4$  precursor flows (0.0, 0.1, and 0.3 sccm). The two data sets were taken at different surface-to-volume ratios:  $1.33 \text{ cm}^{-1}$  (circles) and  $2.04 \text{ cm}^{-1}$  (squares). (The lines merely serve to guide the eye and do not imply a functional interpretation of the data.) The ammonia flow was constant at 10 sccm. Upon addition of  $\text{Ti}(\text{NMe}_2)_4$ , the percent silane reacted clearly increases. For the low surface area case, 9.3% of the silane has reacted upon addition of 0.1 sccm of  $\text{Ti}(\text{NMe}_2)_4$ . This increases to 21.3% for 0.3 sccm of  $\text{Ti}(\text{NMe}_2)_4$ . The data also suggest that the extent of silane reaction per unit  $\text{Ti}(\text{NMe}_2)_4$  decreases with increasing  $\text{Ti}(\text{NMe}_2)_4$ . In other words, the slope of the curve in

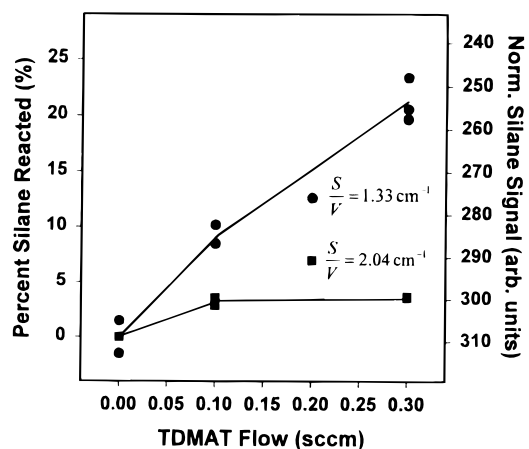


**Figure 2.** Silane mass spectrometer signal (at  $m/e = 30$ ) as a function of  $\text{Ti}(\text{NMe}_2)_4$  flow during the CVD of Ti-Si-N from  $\text{Ti}(\text{NMe}_2)_4 + \text{NH}_3 + \text{SiH}_4$ . The reactor conditions are as follows:  $T = 450 \text{ }^\circ\text{C}$ ;  $P = 6.5 \text{ Torr}$ ;  $\text{NH}_3$  flow =  $\text{SiH}_4$  flow = 10 sccm; residence  $t = 35 \text{ ms}$ . The circles are for  $S/V = 1.33 \text{ cm}^{-1}$  and the squares are for  $S/V = 2.04 \text{ cm}^{-1}$ . The lines serve only to guide the eyes.

**Table 1.** Percent (%) Silane Reacted as a Function of  $\text{Ti}(\text{NMe}_2)_4$  Flow and  $S/V$  for the Reaction of  $\text{Ti}(\text{NMe}_2)_4 + \text{SiH}_4 + \text{NH}_3$ <sup>a</sup>

TMT flow scc/ min	mmol/ min	$S/V = 1.33 \text{ cm}^{-1}$		$S/V = 2.04 \text{ cm}^{-1}$	
		silane <sub>R</sub> / TMT	% silane reacted	silane <sub>R</sub> / TMT	% silane reacted
0.00	0.0000	0.0	0.0	0.0	0.0
0.10	0.0045	9.3	9.3	3.2	3.2
0.30	0.0134	7.1	21.3	1.2	3.7

<sup>a</sup> The reactor conditions are as follows:  $T = 450 \text{ }^\circ\text{C}$ ;  $P = 6.5 \text{ Torr}$ ;  $\text{NH}_3$  flow =  $\text{SiH}_4$  flow = 10 sccm; residence  $t = 35 \text{ ms}$ .

Figure 2 decreases with  $\text{Ti}(\text{NMe}_2)_4$  flow. Table 1 expresses the moles of silane reacted per mole of  $\text{Ti}(\text{NMe}_2)_4$  used in the flow (silane<sub>R</sub>/TDMAT). This ratio decreased from 9.1 to 7.1 as the  $\text{Ti}(\text{NMe}_2)_4$  flow was tripled from 0.10 to 0.30 sccm, suggesting that less silane reacts per unit  $\text{Ti}(\text{NMe}_2)_4$  as more  $\text{Ti}(\text{NMe}_2)_4$  is used in the process. Another interesting aspect of the ratios in Table 1 is that each  $\text{Ti}(\text{NMe}_2)_4$  molecule is capable of activating or reacting with more than one silane molecule.

To estimate the contribution of a heterogeneous component toward silane reactivity, the surface-to-

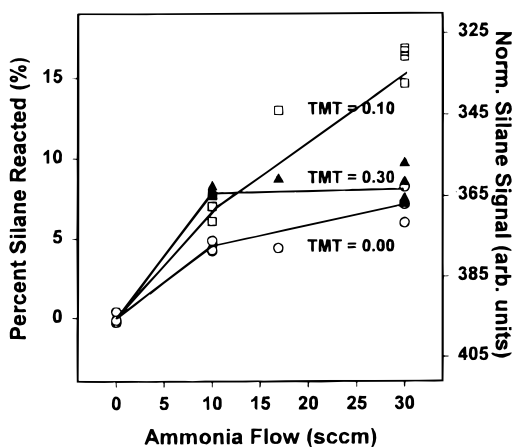


**Figure 3.** Silane mass spectrometer signal (at  $m/e = 30$ ) as a function of  $NH_3$  flow during the CVD of Ti–Si–N from  $Ti(NMe_2)_4 + NH_3 + SiH_4$ . The reactor conditions are as follows:  $T = 450\text{ }^\circ\text{C}$ ;  $P = 6.5\text{ Torr}$ ;  $SiH_4$  flow = 10 sccm; residence  $t = 35\text{ ms}$ . The circles are with TDMAT = 0.0 sccm, the squares with TDMAT = 0.1 sccm, and the triangles with TDMAT = 0.3 sccm. The lines serve only to guide the eyes.

**Table 2. Percent (%) Silane Reacted as a Function of  $Ti(NMe_2)_4$  Flow and  $NH_3$  Flow for the Reaction of  $Ti(NMe_2)_4 + SiH_4 + NH_3^a$**

$NH_3$ flow (sccm)	TMT flow (sccm)		
	0.0	0.1	0.3
0.00	0.00	0.00	0.00
10.00	4.46	6.94	7.92
30.00	7.67	16.09	8.21

<sup>a</sup> The reactor conditions are as follows:  $T = 450\text{ }^\circ\text{C}$ ;  $P = 6.5\text{ Torr}$ ;  $SiH_4$  flow = 10 sccm; residence  $t = 35\text{ ms}$ .

volume (S/V) ratio of the reactor was increased by using a quartz insert. Figure 2 shows that the extent of silane reaction decreases significantly at the higher S/V ratio. This implies that silane reactivity occurs predominantly in the gas phase and in fact, is inhibited by large surface areas. One possible explanation for this is that the larger surface area adsorbs more  $Ti(NMe_2)_4$ , thus making it unavailable for gas-phase reaction with silane.

Figure 3 shows the percent silane reacted as a function of  $NH_3$  flow (0, 10, and 30 sccm) for various  $Ti(NMe_2)_4$  flows: 0.0 (squares), 0.1 sccm (circles), and 0.3 sccm (triangles). (The lines serve only to guide the eye.) Silane reacts to a small extent (Table 2) in the presence of  $NH_3$  with no  $Ti(NMe_2)_4$ . Addition of 0.1 sccm of  $Ti(NMe_2)_4$  increases the extent of silane reaction compared to the no  $Ti(NMe_2)_4$  situation for all ammonia flows. At 0.1 sccm of  $Ti(NMe_2)_4$  and 10 sccm of ammonia, 6.9% of the silane reacts and this increases to 16% at 30 sccm of ammonia. Surprisingly, an increase in  $Ti(NMe_2)_4$  to 0.3 sccm does not further increase the percent silane reacted. Rather, the percent silane reacted at 0.3 sccm of  $Ti(NMe_2)_4$  drops back down to 8.2% at 30 sccm of ammonia. This is the approximately the same extent of reaction that occurred at 0.1 sccm  $Ti(NMe_2)_4$  and 10 sccm ammonia. It is interesting to note that the ratio of  $Ti(NMe_2)_4$  to ammonia is the same for these two cases, i.e., 0.3 sccm  $Ti(NMe_2)_4$ :30 sccm ammonia equals 0.1 sccm  $Ti(NMe_2)_4$ :10 sccm ammonia.

This suggests that the extent of silane reaction is dependent on the relative amounts of  $Ti(NMe_2)_4$  and ammonia.

To determine how well these silane reactivity studies correlate with silicon incorporation into thin films, we deposited Ti–Si–N films in a separate hot-wall thermal CVD reactor. Table 3 shows the atomic composition of these films. The deposition conditions in Table 3 are the same as those in the molecular beam experiments, except for reactor pressure which was 20 Torr compared to 6.5 Torr for the beam experiments. The atomic compositions were determined by X-ray photoelectron spectroscopy (XPS) and confirmed by Rutherford back-scattering spectrometry (RBS).

The Si:Ti ratio in the films decreases from 1.03 to 0.6 as  $Ti(NMe_2)_4$  is increased in the presence of 10 sccm ammonia. This behavior is repeated at 30 sccm ammonia, in which the Si:Ti ratio decreases from 1.38 to 0.55 as  $Ti(NMe_2)_4$  is increased. These results are consistent with the molecular beam mass spectrometry studies in which the silane reacted per unit  $Ti(NMe_2)_4$  decreased when  $Ti(NMe_2)_4$  was increased from 0.1 to 0.3 sccm. For constant  $Ti(NMe_2)_4$  at 0.1 sccm, the Si:Ti ratio increases from 1.03 to 1.38 as ammonia is increased. In contrast, at  $Ti(NMe_2)_4$  equal to 0.3 sccm, the change in the Si:Ti ratio is negligible (0.6 to 0.55) as ammonia is increased. These changes in Si:Ti ratio are also in agreement with how the extent of silane reaction varied with ammonia flow in the molecular beam experiments.

## Discussion

An interpretation of this combination of silane reactivity and thin-film deposition studies is that  $Ti(NMe_2)_4$  activates silane in the presence of  $NH_3$ , allowing silicon to become incorporated into the growing films. A possible mechanism for silane activation by  $Ti(NMe_2)_4$  and ammonia involves formation of some type of titanium imido complex. Previously Cundari et al. have performed ab initio studies of silane (and methane) activation by group IVB imido complexes, including  $H_2Ti=NH$ .<sup>17</sup> They determined the activation of silane by  $H_2Ti=NH$  to be exothermic with  $\Delta H_{rxn} = -2.0\text{ kcal mol}$ . The reaction involves a four-center transition state with an agostic interaction between the metal and the Si–H bond.

The existence of titanium imido complexes is also supported by experimental evidence in the literature.<sup>14a,c,15,18–24</sup> The gas-phase kinetic studies of  $Ti(NMe_2)_4$  and  $NH_3$  by Weiler are particularly relevant because they support the presence of titanium imido complexes, such as  $Ti(=NH)(NMe_2)_2$ , resulting from ammonia transamination and successive dimethylamine eliminations (eqs 1 and 2).<sup>15</sup>



Infrared spectroscopic evidence also supports the formation of imido complexes from  $Ti(NMe_2)_4$  and ammonia.<sup>14a,c</sup> Imido complexes are also implicated as intermediates during the CVD of TiN from precursors made from  $TiCl_4$  and alkylamines.<sup>18</sup> There are related

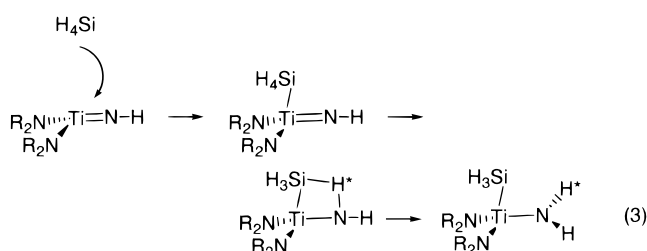
(17) (a) Cundari, T. R. *J. Am. Chem. Soc.* **1992**, *114*, 10557–10563. (b) Cundari, T. R.; Gordon, M. S. *J. Am. Chem. Soc.* **1993**, *115*, 4210–4217. (c) Cundari, T. R.; Morse, J. M. *Chem. Mater.* **1996**, *8*, 189–196.

**Table 3. Composition of Ti–Si–N Films Made by CVD Using Conditions of Molecular Beam Experiments (% = atomic percent)**

<i>T</i> (°C)	<i>P</i> (Torr)	residence <i>t</i> (ms)	silane flow (sccm)	TMT flow (sccm)	NH <sub>3</sub> flow (sccm)	Si/Ti	%Si	%Ti	%N	%C	%O
450	20	35	10	0.1	10	1.03	27	17	35	8	14
450	20	35	10	0.3	10	0.6	17	28	31	9	15
450	20	35	10	0.1	30	1.38	23	17	33	3	25
450	20	35	10	0.3	30	0.55	16	29	34	8	12

examples of titanium alkylimido compounds from solution studies.<sup>19–22</sup> Other transition metals, such as tantalum and zirconium, form alkylimido complexes.<sup>22–24</sup> In fact, it has been demonstrated that the zirconium alkylimido compound activates methane<sup>24</sup> in a manner similar to the activation of methane and silane by titanium imido complexes studied by Cundari.<sup>17</sup>

On the basis of these previous observations as well as the results presented here, it is reasonable to postulate that the first step of silane activation occurs according to the following mechanism:



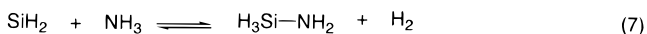
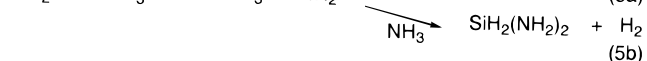
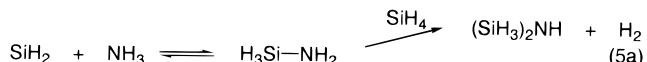
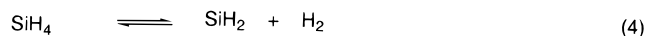
The imido species is generated according to mechanisms 1 and 2 above. The silane activation step is an addition of the Si–H bond across the Ti=N bond through the four-center transition state described by Cundari.<sup>17</sup>

Although not conclusive, this mechanism is consistent with our silane reactivity studies. Increasing Ti(NMe<sub>2</sub>)<sub>4</sub> causes more silane to react by increasing the amount of the imido complex available. If incomplete transamination of Ti(NMe<sub>2</sub>)<sub>4</sub> is assumed under the conditions of these flow experiments, the mechanism also explains why increasing ammonia did not increase silane reactivity for the case of 0.3 sccm Ti(NMe<sub>2</sub>)<sub>4</sub>. There was insufficient ammonia relative to the increased Ti(NMe<sub>2</sub>)<sub>4</sub>. In fact, 0.3 sccm Ti(NMe<sub>2</sub>)<sub>4</sub> and 30 sccm ammonia are the same relative ratio as 0.1 sccm Ti(NMe<sub>2</sub>)<sub>4</sub> and 10 sccm ammonia. This suggests that silane may react more readily with a doubly or triply transaminated titanium–imido species with less steric bulk. If complete transamination is assumed the role of ammonia in silane activation becomes less clear. A titanium–imido species may activate more than one silane molecule, although it remains to be determined

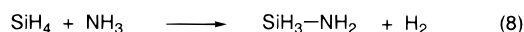
how each TDMAT molecule can activate seven or more silane molecules, according to the data in Table 1. Of course, some of these observations could be related to surface processes.

The decrease in silane reactivity with higher surface area implies that silane activation occurs predominantly in the gas phase. This can be rationalized on the basis of constrained motion of titanium imido complexes that are adsorbed on a surface. The mechanism shown in eq 3 requires lengthening of the Si–H bond, changing direction of the N–H\*–Si angle and increasing in the Ti–N–H\* angle, transfer of H\* to the incipient amido, and pivoting of the amido ligand once it is formed. This sequence of molecular motions is likely to be hindered if they occur on an imido species attached to a surface. Alternatively, higher surface areas may hinder a gas-phase reaction required prior to the silane addition step. It is known from surface studies between 300 and 500 K that TiN deposition occurs only if Ti(NMe<sub>2</sub>)<sub>4</sub> and NH<sub>3</sub> react in the gas phase.<sup>14a</sup> No surface reaction was seen when Ti(NMe<sub>2</sub>)<sub>4</sub> was added to adsorbed NH<sub>3</sub>, or when NH<sub>3</sub> was added to adsorbed Ti(NMe<sub>2</sub>)<sub>4</sub>. This suggests that increased surface area would hinder the gas-phase reaction between Ti(NMe<sub>2</sub>)<sub>4</sub> and NH<sub>3</sub> required to form the imido complex that most likely reacts with silane.

There is an alternative mechanism involving various silicon–nitrogen compounds which may explain the increased silane decomposition upon addition of Ti(NMe<sub>2</sub>)<sub>4</sub> in the presence of ammonia. Silylene, SiH<sub>2</sub>, is a product of silane pyrolysis (eq 4).<sup>25–28</sup> Its various reactions with ammonia to form aminosilane (H<sub>3</sub>Si–NH<sub>2</sub>), silanimine (H<sub>2</sub>Si=NH), and aminosilylene (HSi–NH<sub>2</sub>) have been characterized by ab initio methods (eqs 5–7).<sup>29–32</sup> The direct reaction of silane and ammonia



to form H<sub>3</sub>Si–NH<sub>2</sub> has also been studied theoretically (eq 8).<sup>33</sup> These reactions (eqs 5–8) would explain the



(18) (a) Winter, C. H.; Sheridan, P. H.; Lewkebandara, T. S.; Heeg, M. J.; Proscia, J. W. *J. Am. Chem. Soc.* **1992**, *114*, 1095–1097. (b) Lewkebandara, T. S.; Sheridan, P. H.; Heeg, M. J.; Rheingold, A. L.; Winter, C. H. *Inorg. Chem.* **1994**, *33*, 5879–5889.

(19) Hill, J. E.; Profflet, R. D.; Fanwick, P. E.; Rothwell, I. P. *Angew. Chem., Int. Ed. Engl.* **1990**, *29*, 664–665.

(20) Roesky, H. W.; Voelker, H.; Witt, M.; Noltemeyer, M. *Angew. Chem., Int. Ed. Engl.* **1990**, *29*, 669–670.

(21) Cummins, C. C.; Schaller, C. P.; Van Duyne, G. D.; Wolczanski, P. T.; Chan, A. W. E.; Hoffman, R. *J. Am. Chem. Soc.* **1991**, *113*, 2985–2994.

(22) Nugent, W. A.; Haymore, B. L. *Coord. Chem. Rev.* **1980**, *31*, 123–175.

(23) Nugent, W. A.; Harlow, R. L. *J. Chem. Soc., Chem. Commun.* **1978**, 579–580.

(24) Cummins, C. C.; Baxter, S. M.; Wolczanski, P. T. *J. Am. Chem. Soc.* **1988**, *110*, 8731–8733.

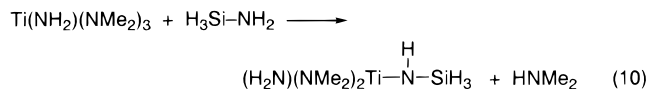
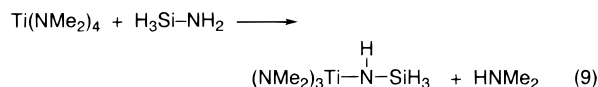
(25) Neudorfl, P.; Jodhan, A.; Strausz, O. P. *J. Phys. Chem.* **1980**, *84*, 338–339.

(26) Ring, M. A.; Puentes, M. J.; O'Neal, H. E. *J. Am. Chem. Soc.* **1970**, *92*, 4845–4848.

(27) Roenigk, K. F.; Jensen, K. F.; Carr, R. W. *J. Phys. Chem.* **1987**, *91*, 5732–5739.

small amount of silane reactivity we observed in the presence of ammonia alone at 450 °C. The relatively low temperature prevents significant amounts of  $SiH_2$  from being produced from the gas-phase decomposition of silane according to published rate data; unless this is somehow facilitated by a Ti-rich surface.<sup>34</sup>

These silicon–nitrogen compounds may undergo transamination reactions with  $Ti(NMe_2)_4$  or similar species (eqs 9 and 10). Steric hindrance may render these



reactions less likely than the titanium imido activation discussed previously. Studies are in progress to determine the occurrence of these two mechanisms during CVD of Ti–Si–N.

(28) Ho, P.; Coltrin, M. E.; Binkley, J. S.; Melius, C. F. *J. Phys. Chem.* **1985**, *89*, 4647–4654.

(29) Melius, C. F.; Allendorf, M. D.; Colvin, M. E. *Electrochem. Soc. Proc.* **1997**, *97–25*, 1–14.

(30) Truong, T. N.; Gordon, M. S. *J. Am. Chem. Soc.* **1986**, *108*, 1775–1778.

(31) Raghavachari, K.; Chandrasekhar, J.; Gordon, M. S.; Dykema, K. J. *J. Am. Chem. Soc.* **1984**, *106*, 5853–5859.

(32) Melius, C. F.; Ho, P. *J. Phys. Chem.* **1991**, *95*, 1410–1419.

(33) (a) Tachibana, A.; Kurosaki, Y.; Sera, T.; Tanaka, E.; Fueno, H.; Yamabe, T. *J. Phys. Chem.* **1990**, *94*, 5234–5240. (b) Tachibana, A.; Kurosaki, Y. *Acta Chim. Hung.* **1993**, *130*, 111–128.

(34) Roenigk, K. F.; Jensen, K. F.; Carr, R. W. *J. Phys. Chem.* **1987**, *91*, 5732–5739.

Attempts to observe this silane reactivity at lower temperatures with the molecular beam mass spectrometer have been unsuccessful to date. This is attributed to the high activation barrier for the reaction of silane with titanium imido complexes. Cundari calculated the enthalpy of activation for this process to be  $\Delta H^\ddagger = 15.5$  kcal/mol, which is significantly higher than the enthalpic barrier of  $\Delta H^\ddagger = 6.9$  kcal/mol for the transamination reaction of  $Ti(NMe_2)_4$  with ammonia, measured by Weiler.<sup>7b,8b</sup> We are in the process of improving the sensitivity of the apparatus to observe this reaction at lower temperatures.

### Conclusions

The most important result from this work is the observation that  $Ti(NMe_2)_4$  activates silane in the presence of ammonia at 450 °C. The extent of silane reaction is dependent upon the relative amounts of  $Ti(NMe_2)_4$  and ammonia. Moreover, Ti–Si–N thin films have been deposited in which the variations of the Ti:Si ratio with  $Ti(NMe_2)_4$  and ammonia flows are consistent with observations of silane reactivity under similar conditions. This demonstrates that knowledge of the gas-phase mechanisms that occur during CVD of Ti–Si–N ultimately can be useful as a means of controlling film composition. Further experiments are underway to further elucidate the mechanism and kinetics of this reaction.

**Acknowledgment.** The authors are grateful for financial support provided by the National Science Foundation (DMR-9631794 and DMR-9875062) and the University of New Hampshire.

CM990174J